

# Solution Processed Low Voltage Metal-Oxide transistor by using $\text{TiO}_2$ / $\text{Li-Al}_2\text{O}_3$ stacked Gate Dielectric

**Nila Pal**

Indian Institute of Technology Banaras Hindu University: Indian Institute of Technology BHU Varanasi

**Utkarsh Pandey**

Indian Institute of Technology Banaras Hindu University: Indian Institute of Technology BHU Varanasi

**Sajal Biring**

Ming Chi University of Technology

**Bhola Nath Pal** (✉ [bnpal.mst@iitbhu.ac.in](mailto:bnpal.mst@iitbhu.ac.in))

Indian Institute of Technology Banaras Hindu University: Indian Institute of Technology BHU Varanasi

<https://orcid.org/0000-0001-7512-3441>

---

## Research Article

**Keywords:** Solution process, Metal oxide semiconductor, Ion-conducting gate dielectric, Bilayer stack dielectric, TFT, Schottky junction

**Posted Date:** May 11th, 2021

**DOI:** <https://doi.org/10.21203/rs.3.rs-350224/v1>

**License:**  This work is licensed under a Creative Commons Attribution 4.0 International License.

[Read Full License](#)

---

**Version of Record:** A version of this preprint was published at Journal of Materials Science: Materials in Electronics on January 29th, 2022. See the published version at <https://doi.org/10.1007/s10854-021-07581-z>.

# Abstract

A solution processed top-contact bottom gated SnO<sub>2</sub> thin-film transistor (TFT) has been fabricated by using a TiO<sub>2</sub>/ Li-Al<sub>2</sub>O<sub>3</sub> bilayer stacked gate dielectric that show operating voltage of this TFT within 2.0 V. It is observed that the bilayer dielectric has much higher areal capacitance with lower leakage current density that significantly improve the overall device performance of TFT. The TFT with bilayer gate dielectric shows an effective carrier mobility ( $\mu_{\text{sat}}$ ) of 9.2 cm<sup>2</sup>V<sup>-1</sup>s<sup>-1</sup> with an on/off ratio of 7.1x10<sup>3</sup> which are significantly higher with respect to the TFT with a single layer Li-Al<sub>2</sub>O<sub>3</sub> gate dielectric. The origin of this improvement is due to the Schottky junction between the highly doped silicon (p<sup>++</sup>-Si) and TiO<sub>2</sub> of bilayer stacked dielectric that induced electrons to the channel which reduces the dielectric/semiconductor interface trap state. This investigation opens a new path to develop TFT device performance using a suitable bilayer stack of gate-dielectric.

## 1. Introduction

The charge carrier conduction of the channel of a thin film transistor (TFT) normally occurs within < 10 nm thickness of the semiconductor film next to the gate-dielectric.<sup>1</sup> Therefore, the field effect charge transport phenomena of a TFT is not only dependent on the microstructures of the semiconductor but is also strongly affected by the surface properties of the gate-insulator. Conventional silicon gate dielectric (SiO<sub>2</sub>) commonly offers smooth surface morphology which is capable of minimizing the defect density of semiconductor-insulator interface. However, the dielectric constant of SiO<sub>2</sub> is very low (3.9). Therefore, to reduce the operating voltage of a TFT below 2 V for portable electronics application, it requires very low thickness of SiO<sub>2</sub> (< 10 nm) which sometime becomes very licky.<sup>2,3</sup> Employment of high-k dielectric materials instead of SiO<sub>2</sub> is the best alternative which allow us to deposit thicker dielectric film by maintaining the advantage of low operating voltage TFT fabrication.<sup>4,5,6,7,8</sup> However, ionic bonds in high-k dielectrics results in high defect concentrations with oxygen vacancies (V<sub>O</sub>) being the primary source of traps. These can be source of fixed charges or act as electron traps, scattering carriers in channel (decreasing mobility), changing the threshold voltage (V<sub>T</sub>) and assisting dielectric breakdown and gate-leakage mechanism,<sup>9</sup> decreasing device performance, and affects the stability and reliability of devices. To overcome these problems different approaches like inorganic-organic hybrid dielectric,<sup>10</sup>{Canimkurbey, 2019 #81} Ta<sub>2</sub>O<sub>5</sub>/SiO<sub>2</sub> multicomponent dielectric,<sup>11</sup> bilayer-dielectric stack<sup>12,13,14</sup>, have been used. A new method to reduce the semiconductor-insulator interface trap-states is found by implying n-type TiO<sub>2</sub> as interface layer between highly doped silicon (p<sup>++</sup>-Si) substrate and high-k ion conducting Li<sub>5</sub>AlO<sub>4</sub> dielectric, which drastically enhance the TFT device performance due to the formation of Schottky junction of p<sup>++</sup>-Si/TiO<sub>2</sub>.<sup>15</sup> However, capacitance of this Li<sub>5</sub>AlO<sub>4</sub>/TiO<sub>2</sub> stacked dielectric reduce rapidly > 10<sup>4</sup> Hz. To enhance this frequency range and overall performance of TFT, more detailed study is required for different combinations of stacked dielectric.

In this work, we have synthesized Li-doped alumina ( $\text{Li-Al}_2\text{O}_3$ ) thin film by sol-gel method and have used this ionic dielectric to fabricate  $\text{TiO}_2$  / $\text{Li-Al}_2\text{O}_3$  stacked gate dielectric. The variation of areal capacitance of this bilayer stacked gate dielectric only 20% up to the frequency  $10^5$  Hz. To realize the overall improvement of TFT performance and the mechanism of this development, two sets of solution processed  $\text{SnO}_2$  TFT were fabricated; one with  $\text{TiO}_2$  gate interface and another without gate interface. Comparative studies of these two TFT reveals a significant improvement of device performance. A schematic presentation of energy band gap of multilayer thin films and related charge transfer of  $\text{p}^{++}$ - $\text{Si}/\text{TiO}_2$  Schottky junction explain the probable reason for enhancing device performance.

## 2. Experimental

### 2.1 Material Synthesis

As mentioned earlier, all TFTs are fabricated by low-cost solution processed technique. In this process, both gate dielectric ( $\text{TiO}_2$  and  $\text{Li-Al}_2\text{O}_3$ ) and semiconducting layers ( $\text{SnO}_2$ ) are deposited from the precursor solution by spin coating method. For  $\text{TiO}_2$  deposition, a solution of 100 mM was prepared by dissolving Titanium(IV) Butoxide in 2-methoxy ethanol (2ME) followed at the room temperature stirring process by a magnetic stirrer about 30 minutes. Similarly, to prepare the  $\text{Li-Al}_2\text{O}_3$  dielectric, two different solutions of lithium acetate and aluminium nitrate nonahydrate of concentration 500 mM were prepared by using 2-methoxy ethanol as solvent. These two homogeneous solutions are mixed with a ratio of 1:11 to maintain the atomic ratio of the final product of  $\text{Li-Al}_2\text{O}_3$ . This mixture of solutions was left for 24 hours for proper gelation before deposition.<sup>16</sup> Finally, solution was filtered by 0.45  $\mu\text{m}$  PVDF filter before spin coating. For semiconductor ( $\text{SnO}_2$ ) thin film deposition, a solution of  $\text{SnCl}_2$  has been prepared by using 2-methoxy ethanol as solvent.

### 2.2 Device Fabrication

Metal-Oxide TFTs are fabricated in a top-contact bottom-gate configuration by using highly p-doped Si wafer ( $\text{p}^{++}$ -Si) as a substrate as well as gate electrode. Initially, all the Si wafers are cleaned with standard cleaning process. After wet cleaning, wafers were treated with an oxygen plasma for 10 minutes before spin coating. Plasma treatment makes the surface hydrophilic which increases the adhesive property and helps to form pinhole free smooth film during spin coating. Two types of devices are fabricated without and with  $\text{TiO}_2$  interface named as Device 1 and Device 2 shown in Fig. 1a and b, respectively. The  $\text{TiO}_2$  thin film is deposited on  $\text{p}^{++}$ -Si wafer spin coating with a spinning speed of 3500 rpm for 40 seconds followed by a drying process of a preheated hot-plate (set at  $90^\circ\text{C}$ ) to evaporate the solvent. Afterwards, this film was annealed at  $350^\circ\text{C}$  for 30 minutes to form a polycrystalline thin film of  $\text{TiO}_2$ . On top of this, the precursor solution of  $\text{Li-Al}_2\text{O}_3$  was spin coated with a speed 5000 rpm for 50s followed by annealing process at  $350^\circ\text{C}$  for 30 minute. The dielectric film coating was repeated three times to achieve a desired thickness of the dielectric layer. Finally this film was annealed at  $500^\circ\text{C}$  for one hour to form  $\text{Li-Al}_2\text{O}_3$  thin film. For Device 1, the same procedure was followed except the  $\text{TiO}_2$  layer deposition. After dielectric

deposition, the precursor solution of SnO<sub>2</sub> was spin coated (4000 rpm for 40 sec.) and subsequent annealing (500°C for 30 minute) process.<sup>17</sup> Finally, aluminium source/drain electrode are deposited by thermal evaporation method with width-to-length ratio of 118. In addition to this TFT fabrication, the metal-insulator-metal (MIM) devices (Fig. 1c and d) were fabricated in a similar process for the electrical characterization of single and bilayer dielectric thin films.

## 2.3 Material and Device characterization

Crystal phase/structural analysis of thin films were carried out by grazing incidence XRD (Rikagu, Smart Lab) with monochromatized Cu K $\alpha$  radiation ( $\lambda = 1.5405 \text{ \AA}$ ). Atomic force microscopy (AFM) study has been performed by using "NTMDTNTTEGRA-prima" to measure the roughness of different thin film surfaces. Thin films are deposited on p<sup>++</sup>-Si substrate in both cases. Frequency vs. Capacitance (C-f) measurement has been done by LCR meter (keysight LCR meter E4990A). All the electrical characteristics of TFTs and leakage current measurement of MIM devices have been measured by semiconductor parameter analyzer (KEYSIGHT B1500A).

## 3. Results And Discussions

### 3.1 Grazing Incidence X-Ray Diffraction Pattern of Thin Films

To analyse the structural properties of spin coated TiO<sub>2</sub>, Li-Al<sub>2</sub>O<sub>3</sub> and SnO<sub>2</sub> thin film, individually all these thin films were deposited on p<sup>++</sup>-Si substrate under the same condition of TFT fabrication. Figure 2a shows the GIXRD patterns of TiO<sub>2</sub> thin film which indicates a crystalline peak at  $2\theta \sim 25.28^\circ$ , which is corresponding to the (101) plane of stable anatase phase of TiO<sub>2</sub>. The GIXRD patterns of Li-Al<sub>2</sub>O<sub>3</sub> dielectric which is shown in Fig. 2b, didn't show any diffraction peak, indicating the amorphous nature of Li-Al<sub>2</sub>O<sub>3</sub> dielectric.

The GIXRD pattern of SnO<sub>2</sub> thin film has been shown in Fig. 2c that clearly identified diffraction peaks at the  $2\theta$  angle 26.6, 34.2, 52.7, and 54.7 which are corresponds the reflection planes of (110), (101), (211) and (220) respectively; justify the tetragonal phase of SnO<sub>2</sub> (JCPDS 88-0287).

### 3.2 Surface Morphology of Dielectric Thin Films

The surface morphologies of single layer Li-Al<sub>2</sub>O<sub>3</sub> and bilayer TiO<sub>2</sub>/Li-Al<sub>2</sub>O<sub>3</sub> dielectrics were studied by atomic force microscopy (AFM). All these dielectric layers were deposited on p<sup>++</sup>-Si substrates with the same condition as for TFT fabrication. The 2-D and 3-D morphologies of these two dielectric thin films are shown in Fig. 3a and 4b represent the AFM images of Li-Al<sub>2</sub>O<sub>3</sub> dielectric whereas, Fig. 3c and 4d are AFM pictures of TiO<sub>2</sub>/Li-Al<sub>2</sub>O<sub>3</sub> dielectrics. Figure 3 shows that the RMS roughness of both dielectric thin films are < 1 nm which is suitable for high performance TFT fabrication. However, compared to single layer Li-Al<sub>2</sub>O<sub>3</sub> surface (0.26 nm) a little bit smoother than bilayer TiO<sub>2</sub>/Li-Al<sub>2</sub>O<sub>3</sub> surface (0.46 nm).

### 3.3 Dielectric and Electrical characterization

The leakage current density and areal capacitance of single layer and bilayer dielectric are measured with metal-insulator-metal (MIM) architecture which is shown in Fig. 4. Figure 4a shows the leakage current density vs. applied voltage graphs of both dielectric thin films. This data indicates that stacked dielectric of  $p^{++}\text{-Si}/\text{TiO}_2/\text{Li-Al}_2\text{O}_3/\text{Al}$  device has one order lower leakage current density than  $p^{++}\text{-Si}/\text{Li-Al}_2\text{O}_3/\text{Al}$  device at applied voltage 2 V with a current density of  $6.2 \times 10^{-5} \text{ A/cm}^2$  where as single layer dielectric MIM device shows a current density of  $2.0 \times 10^{-4} \text{ A/cm}^2$  at 2.0 V. The dielectric-leakage current of bilayer film is reasonably low for TFT fabrication that operates within 2.0 V operating voltage. The reduction of gate-leakage current in case of bilayer dielectric may be resulted from the lattice mismatch of two different materials with different grain shapes at the interfaces, which is well understood from the earlier multilayered dielectric studies.<sup>14</sup>

The variation of capacitance per unit area of the same set of MIM devices with frequencies (20 to  $10^5$  Hz) at room temperature are represented in Fig. 4b. It is well known that the capacitance decreases with frequency due to the different relaxation times originated from different types of polarization contribution.<sup>6</sup> Similar behavior is observed in both types of MIM devices that reduce significantly  $> 10^3$ Hz. However, the capacitance of single layer  $p^{++}\text{-Si}/\text{Li-Al}_2\text{O}_3/\text{Al}$  device changes more rapidly compared to bilayer  $p^{++}\text{-Si}/\text{TiO}_2/\text{Li-Al}_2\text{O}_3/\text{Al}$  MIM device. The measured areal capacitance (C) values of single and bilayer MIM devices are  $55 \text{ nF/cm}^2$  and  $66 \text{ nF/cm}^2$  at 50 Hz frequency, respectively. This study is the indication of the higher areal capacitance value with wider frequency range of a bilayer stacked dielectric thin film which originated from additional  $\text{TiO}_2$  layer. The  $\text{TiO}_2/\text{Li-Al}_2\text{O}_3$  bilayer act as series combination of  $\text{TiO}_2$  and  $\text{Li-Al}_2\text{O}_3$  parallel plate capacitor and the resultant capacitance can be written as;

$$\frac{1}{C_{\text{effective}}} = \frac{1}{C_{\text{TiO}_2}} + \frac{1}{C_{\text{Li-Al}_2\text{O}_3}}$$

The high-k value of  $\text{TiO}_2$  layer increases the capacitance of  $\text{TiO}_2/\text{Li-Al}_2\text{O}_3$  dielectric with respect to  $\text{Li-Al}_2\text{O}_3$  single layer.

### 3.4 Electrical Characterization of Single and Bilayer Dielectric Thin Film Transistor

To realize the performance of these dielectric layers for the application of gate dielectric of TFTs, two sets of devices have been fabricated. Device 1 is the reference TFT without  $\text{TiO}_2$  gate interface and Device 2 is TFT with  $\text{TiO}_2$  gate-interface in between gate electrode and  $\text{Li-Al}_2\text{O}_3$  gate-dielectric. A higher channel length of  $200 \mu\text{m}$  with W/L ( $W = 23.6 \text{ mm}$ ,  $L = 0.2 \text{ mm}$ ) ratio of 118 is chosen to avoid the overestimation of carrier mobility value due to grain boundary effect, which is highly dominating below  $25 \mu\text{m}$  channel length and W/L ratio of 10.<sup>17, 18</sup> Additionally, high-performance TFT with larger device area demands good quality of dielectric with pinhole-free uniform thin film with very low defect states. Figure 5 shows

transistor characteristics of two types of device, and are measured at ambient conditions. The  $I_D$ - $V_D$  characteristics of Device 1 and Device 2 are shown in Fig. 5 a and b, respectively. The applied  $V_D$  are swept from 0 to 1V with different constant gate voltages ranging from - 0.2 to 2.0V with step of 0.2V. The linear and saturation region of the output characteristics are clearly shown by the figure for both sets of devices.

The Transfer characteristics of SnO<sub>2</sub> TFT without and with TiO<sub>2</sub> interface are shown in Fig. 5c and d. The gate to source voltages is swept from - 0.2 to 2V keeping  $V_D$  constant at 1V for both devices. All the measurement conditions and parameters are kept the same for all devices. From comparative data of transfer characteristics (Fig. 5e and f), it is observed that the threshold voltage of Device 2 (0.29V) is sufficiently lower than Device 1 (0.85 V). Besides, the calculated value of  $I_{ON}/I_{OFF}$  ratio for Device 2 is  $7.2 \times 10^3$  which is higher than Device 1 (i.e.  $3.6 \times 10^3$ ). The effective carrier mobility ( $\mu$ ), subthreshold swing

(SS) and dielectric/semiconductor interface trap-states ( $N_{SS}^{Max}$ ) of TFT have been calculated by using the following equations.<sup>19</sup>

$$SS = \left[ \frac{d(\log I_D)}{dV_G} \right]^{-1} \dots \dots \dots (1)$$

$$I_D = \mu C \frac{W}{2L} (V_G - V_T)^2 \dots \dots \dots (2)$$

$$N_{SS}^{Max} = \left[ \frac{SS \times \log e}{\frac{kT}{q}} - 1 \right] \frac{C}{q} \dots \dots \dots (3)$$

Where k, T and q are the Boltzmann constant, temperature in absolute scale and charge of electron respectively. The saturation carrier mobilities of both devices are calculated by using Eq. 1 and extracted from the linear fitting of  $(I_D)^{1/2}$  vs.  $V_G$  plot. From comparison of both devices, it is observed that device 2 shows better performance having saturation electron mobility of  $9.2 \text{ cm}^2\text{V}^{-1}\text{s}^{-1}$  than device 1 that shows saturation electron mobility of  $7.7 \text{ cm}^2\text{V}^{-1}\text{s}^{-1}$ . The subthreshold swing (SS) value of both devices are extracted from the slope at lower gate-voltage regime of the  $\log(I_D)$  vs.  $V_G$  graphs (shown in Fig. 5 e and f) and by using Eq. 2. Device 2 has lower SS value (250 mV/decade) than Device 1 (280 mV/decade).

The dielectric-semiconductor interface trap-state densities have been derived from Eq. 3. Device 1 has a 1.5 time higher interface trap-state density than Device 2. The lower  $N_{SS}^{Max}$  leads to less trapping of

charge carriers in the dielectric-semiconductor interface, resulting in improvement of effective mobility and higher drain current.<sup>20</sup> All the TFT parameters are summarized in Table 1.

Table 1 : Summary of the TFT parameters of SnO<sub>2</sub> transistors with single layer and bilayer stack gate-dielectrics.

Device	Threshold Voltage (V)	I <sub>ON</sub> /I <sub>OFF</sub>	Subthreshold Swing (mV/decade)	Saturation Mobility (cm <sup>2</sup> V <sup>-1</sup> s <sup>-1</sup> )	Interface trap-state density (cm <sup>-2</sup> )
Si <sup>++</sup> /Li-Al <sub>2</sub> O <sub>3</sub> /SnO <sub>2</sub> /Al	0.85	3.6x10 <sup>3</sup>	280	7.7	1.6x10 <sup>12</sup>
Si <sup>++</sup> /TiO <sub>2</sub> /Li-Al <sub>2</sub> O <sub>3</sub> /SnO <sub>2</sub> /Al	0.29	7.2x10 <sup>3</sup>	250	9.2	1.1x10 <sup>12</sup>

To understand the reason behind the higher performance of device 2 with TiO<sub>2</sub>/Li-Al<sub>2</sub>O<sub>3</sub> stack dielectric, a schematic diagram of energy bands of two types of SnO<sub>2</sub> TFTs have been illustrated in Fig. 6. Since p<sup>++</sup>-Si(111)/TiO<sub>2</sub> interface forms a Schottky junction at zero gate bias, the electron of TiO<sub>2</sub> layer transferred to the p<sup>++</sup>-Si gate-electrode creates a depleted layer of positive charge at TiO<sub>2</sub> thin film. However, hole is not allowed to transfer from p<sup>++</sup>-Si to TiO<sub>2</sub> layer due to large potential barrier in p<sup>++</sup>-Si(111)/TiO<sub>2</sub> interface.<sup>21,22</sup> Hence, the layer of positive charge of TiO<sub>2</sub> thin film induces electrons of the channel of TFT (SnO<sub>2</sub>) to accumulate at the Li-Al<sub>2</sub>O<sub>3</sub>/SnO<sub>2</sub> interface, which initially fills up the electron trap-states

$(N_{SS}^{Max})$  at the dielectric/semiconductor interface (Fig. 6a).

This phenomenon is happening without gate-bias. Therefore, TiO<sub>2</sub> thin film effectively reduces the interface trap-states, resulting in a lower sub-threshold swing and threshold voltage. Although, this phenomena is not occurring in device 1 because of the high barrier height of insulating Li-Al<sub>2</sub>O<sub>3</sub> layer. Therefore, electrons cannot be ejected from Li-Al<sub>2</sub>O<sub>3</sub> to p<sup>++</sup>-Si gate-electrode (Fig. 6c). Under accumulation mode operation, a positive gate voltage is applied to both of the devices (Fig. 6band d). However, this bias does not change the depletion layer width of p<sup>++</sup>-Si(111)/TiO<sub>2</sub> interface due to the intermediate insulating Li-Al<sub>2</sub>O<sub>3</sub> layer. This phenomena effectively enhances the accumulation of mobile charge carriers in the channel of device 2, that improves the device performance over Device 1.

## 4. Conclusion

In conclusion, high-performance solution processed low operating voltage SnO<sub>2</sub> thin-film transistor has been fabricated onto sol-gel derived ion-conduction Li-Al<sub>2</sub>O<sub>3</sub> dielectric by using TiO<sub>2</sub> gate interface. A comparative study of two sets of SnO<sub>2</sub> TFTs with and without TiO<sub>2</sub> interface have been demonstrated. The Schottky junction formation between p<sup>++</sup>-Si and n-type TiO<sub>2</sub> help to accumulate extra electrons at the Li-Al<sub>2</sub>O<sub>3</sub>/SnO<sub>2</sub> interface, which essentially fills up the interface trap-states and reduces the sub-threshold swing (SS) as well as threshold voltage (V<sub>T</sub>) and enhance the saturation carrier mobility of the device with compared to the device without TiO<sub>2</sub> interface. The high-k value of TiO<sub>2</sub> improves the capacitance of

the TiO<sub>2</sub> / Li-Al<sub>2</sub>O<sub>3</sub> stack dielectric as well as its leakage current also reduced compared to single layered Li-Al<sub>2</sub>O<sub>3</sub> dielectric. We have achieved an effective carrier mobility ( $\mu_{\text{sat}}$ ) of 9.2 cm<sup>2</sup>V<sup>-1</sup>s<sup>-1</sup>, SS of 250 mV/decade, and V<sub>T</sub> of 0.29 V in TiO<sub>2</sub>/ Li-Al<sub>2</sub>O<sub>3</sub> stack TFT with an I<sub>ON</sub>/I<sub>OFF</sub> ratio of 7.2x10<sup>3</sup>. This investigation opens a new path to develop high-performance TFT devices by using a suitable bilayer stack of gate-dielectrics.

## Declarations

### Acknowledgement

This work was supported by the "Science and Engineering Research Board," India (EMR/2015/000689). The authors are grateful to the Central Instrument Facility Centre, IIT (BHU), for providing the AFM measurement facility. Nila Pal thanks DST-SERB for providing SRF fellowship, and Utkarsh Pandey thanks IIT (BHU) for providing Ph.D. fellowship.

**Conflict of interest** The authors declare no competing financial interest.

## References

1. J. Zaumseil, H. Sirringhaus, Electron and ambipolar transport in organic field-effect transistors. *Chemical reviews* **107**(4), 1296–1323 (2007)
2. J. Robertson, R.M. Wallace, High-K materials and metal gates for CMOS applications. *Materials Science and Engineering: R: Reports* **88**, 1–41 (2015)
3. I.R. Committee, International technology roadmap for semiconductors. 2008
4. B.N. Pal, B.M. Dhar, K.C. See, H.E. Katz, Solution-deposited sodium beta-alumina gate dielectrics for low-voltage and transparent field-effect transistors. *Nature materials* 2009, **8** (11), 898
5. N.K. Chourasia, A. Sharma, V. Acharya, N. Pal, S. Biring, B.N. Pal, Solution processed low band gap ion-conducting gate dielectric for low voltage metal oxide transistor. *J. Alloy. Compd.* **777**, 1124–1132 (2019)
6. B. Wang, W. Huang, L. Chi, M. Al-Hashimi, T.J. Marks, A. Facchetti, High-k gate dielectrics for emerging flexible and stretchable electronics. *Chemical reviews* **118**(11), 5690–5754 (2018)
7. A. Sharma, N.K. Chourasia, A. Sugathan, Y. Kumar, S. Jit, S.-W. Liu, A. Pandey, S. Biring, B.N. Pal, Solution processed Li<sub>5</sub>AlO<sub>4</sub> dielectric for low voltage transistor fabrication and its application in metal oxide/quantum dot heterojunction phototransistors. *Journal of Materials Chemistry C* 2018, **6** (4), 790–798
8. A. Sharma, N.K. Chourasia, V. Acharya, N. Pal, S. Biring, S.-W. Liu, B.N. Pal, Ultra-Low Voltage Metal Oxide Thin Film Transistor by Low-Temperature Annealed Solution Processed LiAlO<sub>2</sub> Gate Dielectric. *Electron. Mater. Lett.* **16**(1), 22–34 (2020)



9. S. Mohsenifar, M. Shahrokhbabadi, Gate stack high- $\kappa$  materials for Si-based MOSFETs past, present, and futures. *terminology* 2015, 2, 5
10. Q. Li, S. Li, D. Yang, W. Su, Y. Wang, W. Zhou, H. Liu, S. Xie, Designing hybrid gate dielectric for fully printing high-performance carbon nanotube thin film transistors. *Nanotechnology* 2017, 28 (43), 435203
11. J. Martins, A. Kiazadeh, J.V. Pinto, A. Rovisco, T. Gonçalves, J. Deuermeier, E. Alves, R. Martins, E. Fortunato, P. Barquinha, Ta<sub>2</sub>O<sub>5</sub>/SiO<sub>2</sub> Multicomponent Dielectrics for Amorphous Oxide TFTs. *Electronic Materials* 2(1), 1–16 (2021)
12. J.-W. Jo, K.-H. Kim, J. Kim, S.G. Ban, Y.-H. Kim, S.K. Park, High-mobility and hysteresis-free flexible oxide thin-film transistors and circuits by using bilayer sol–gel gate dielectrics. *ACS Appl. Mater. Interfaces* 10(3), 2679–2687 (2018)
13. K. Pak, J. Choi, C. Lee, S.G. Im, Low-Power, Flexible Nonvolatile Organic Transistor Memory Based on an Ultrathin Bilayer Dielectric Stack. *Advanced Electronic Materials* 5(4), 1800799 (2019)
14. J.-P. Locquet, C. Marchiori, M. Sousa, J. Fompeyrine, J.W. Seo, High-K dielectrics for the gate stack. *J. Appl. Phys.* 100(5), 051610 (2006)
15. A. Sharma, N.K. Chourasia, N. Pal, S. Biring, B.N. Pal, Role of electron donation of TiO<sub>2</sub> gate interface for developing solution-processed high-performance one-volt metal-oxide thin-film transistor using ion-conducting gate dielectric. *The Journal of Physical Chemistry C* 2019, 123 (33), 20278–20286
16. Y. Liu, P. Guan, B. Zhang, M.L. Falk, H.E. Katz, Ion dependence of gate dielectric behavior of alkali metal ion-incorporated aluminas in oxide field-effect transistors. *Chem. Mater.* 25(19), 3788–3796 (2013)
17. K. Okamura, D. Nikolova, N. Mechau, H. Hahn, Appropriate choice of channel ratio in thin-film transistors for the exact determination of field-effect mobility. *Applied Physics Letters* 2009, 94 (18), 183503
18. G. Adamopoulos, A. Bashir, S. Thomas, W.P. Gillin, S. Georgakopoulos, M. Shkunov, M.A. Baklar, N. Stingelin, R.C. Maher, L.F. Cohen, Spray-Deposited Li-Doped ZnO Transistors with Electron Mobility Exceeding 50 cm<sup>2</sup>/Vs. *Advanced materials* 22(42), 4764–4769 (2010)
19. E. Fortunato, P. Barquinha, R. Martins, Oxide semiconductor thin-film transistors: a review of recent advances. *Advanced materials* 2012, 24 (22), 2945–2986
20. C. Zhu, A. Liu, G. Liu, G. Jiang, Y. Meng, E. Fortunato, R. Martins, F. Shan, Low-temperature, nontoxic water-induced high- $\kappa$  zirconium oxide dielectrics for low-voltage, high-performance oxide thin-film transistors. *Journal of Materials Chemistry C* 2016, 4 (45), 10715–10721
21. S. Avasthi, W.E. McClain, G. Man, A. Kahn, J. Schwartz, J.C. Sturm, Hole-blocking titanium-oxide/silicon heterojunction and its application to photovoltaics. *Appl. Phys. Lett.* 102(20), 203901 (2013)
22. J. Jhaveri, A.H. Berg, J.C. Sturm, Isolation of hole versus electron current at p-Si/TiO<sub>2</sub> selective contact using a heterojunction bipolar transistor structure. *IEEE Journal of Photovoltaics* 2018, 8 (3), 726–732

# Figures

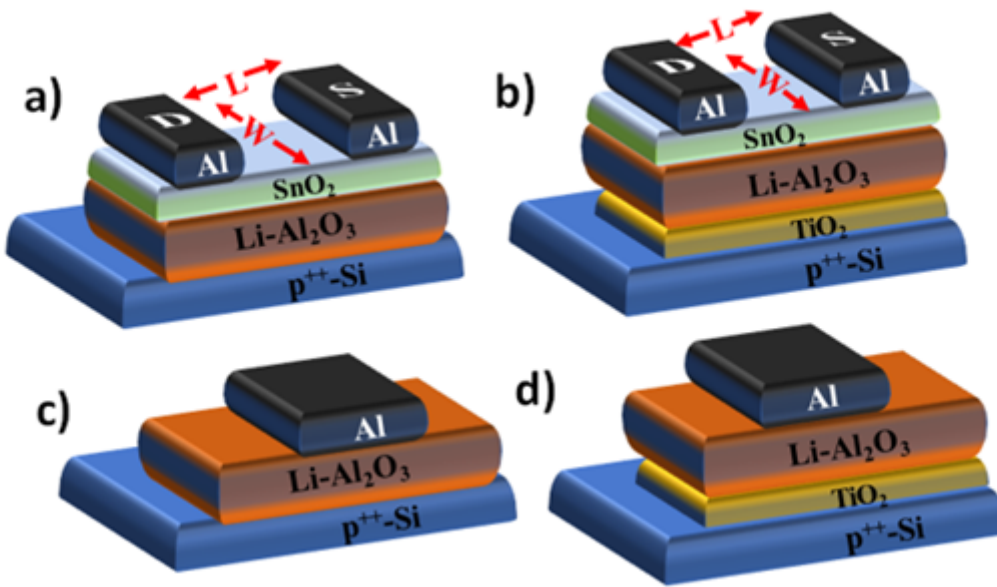


Figure 1

Schematic diagram of TFT devices , a) Device 1 with single layer Li-Al<sub>2</sub>O<sub>3</sub> gate-dielectric, b) Device 2 with bilayer TiO<sub>2</sub>/Li-Al<sub>2</sub>O<sub>3</sub> gate-dielectric. MIM devices with c) Li-Al<sub>2</sub>O<sub>3</sub> gate-dielectric and, d) TiO<sub>2</sub>/Li-Al<sub>2</sub>O<sub>3</sub> gate-dielectric.

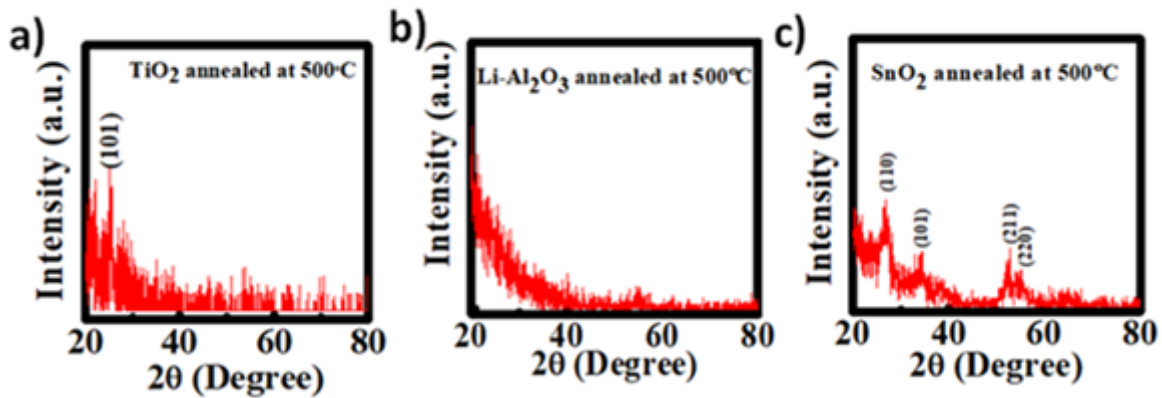


Figure 2

The GIXRD patterns of a) TiO<sub>2</sub>, b) Li-Al<sub>2</sub>O<sub>3</sub> dielectric, and c) SnO<sub>2</sub> semiconductor layer annealed at 500°C.

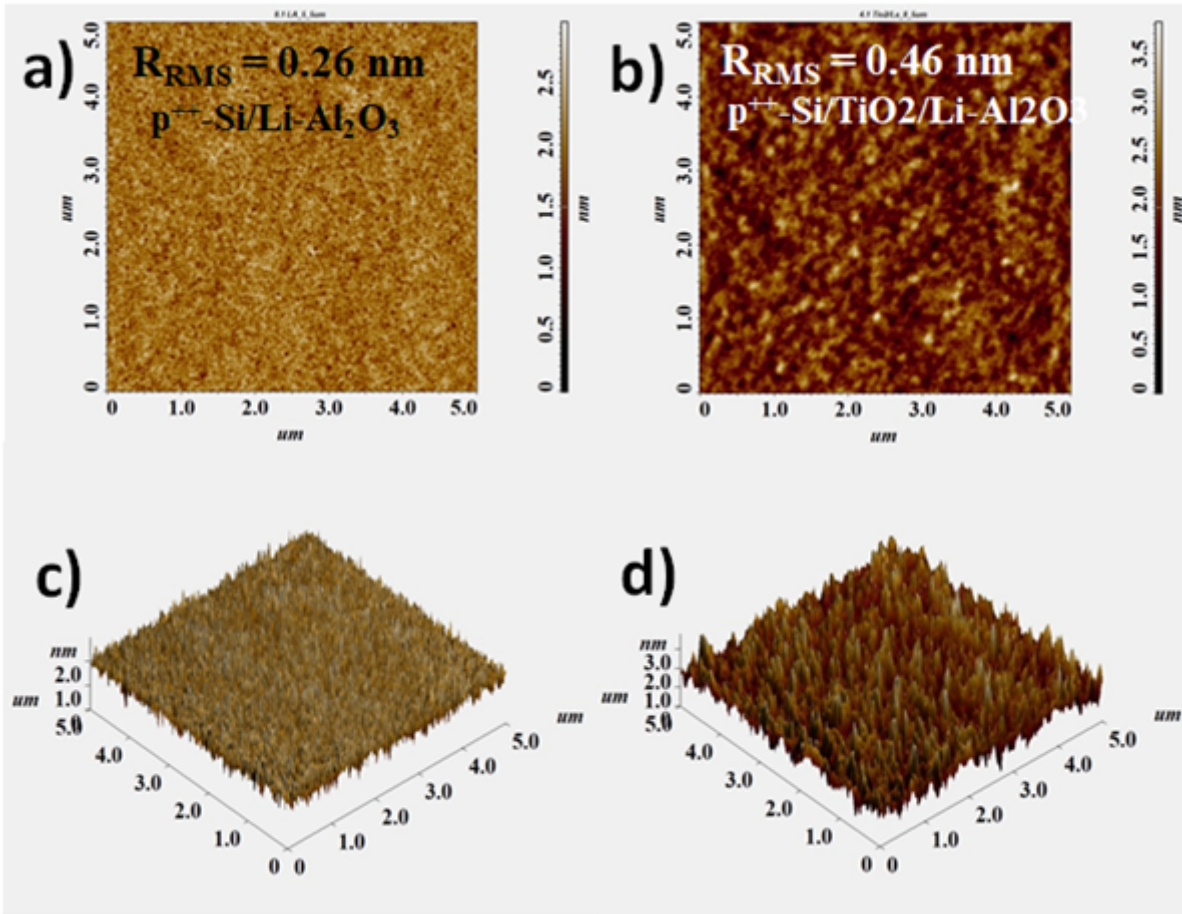


Figure 3

2D AFM image of a) Li-Al<sub>2</sub>O<sub>3</sub> and b) TiO<sub>2</sub>/Li-Al<sub>2</sub>O<sub>3</sub> dielectric. 3D AFM images of c) a) Li-Al<sub>2</sub>O<sub>3</sub> and b) TiO<sub>2</sub>/Li-Al<sub>2</sub>O<sub>3</sub> dielectric.

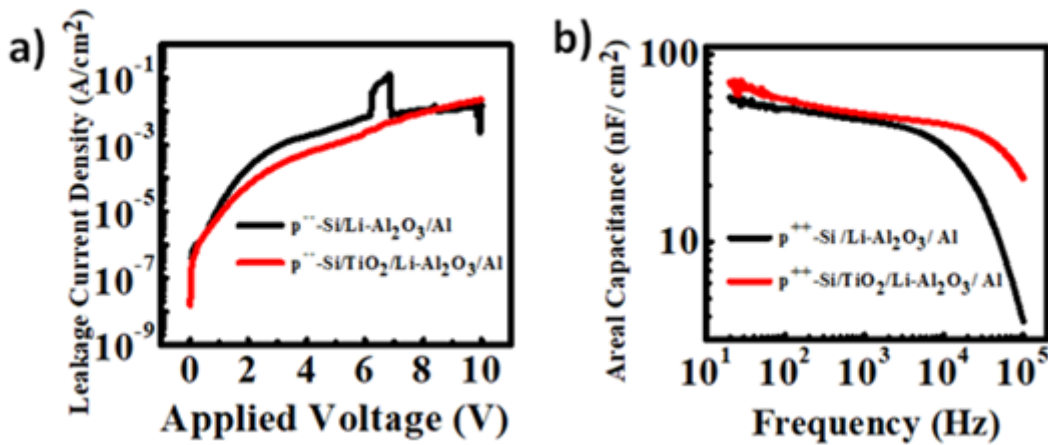
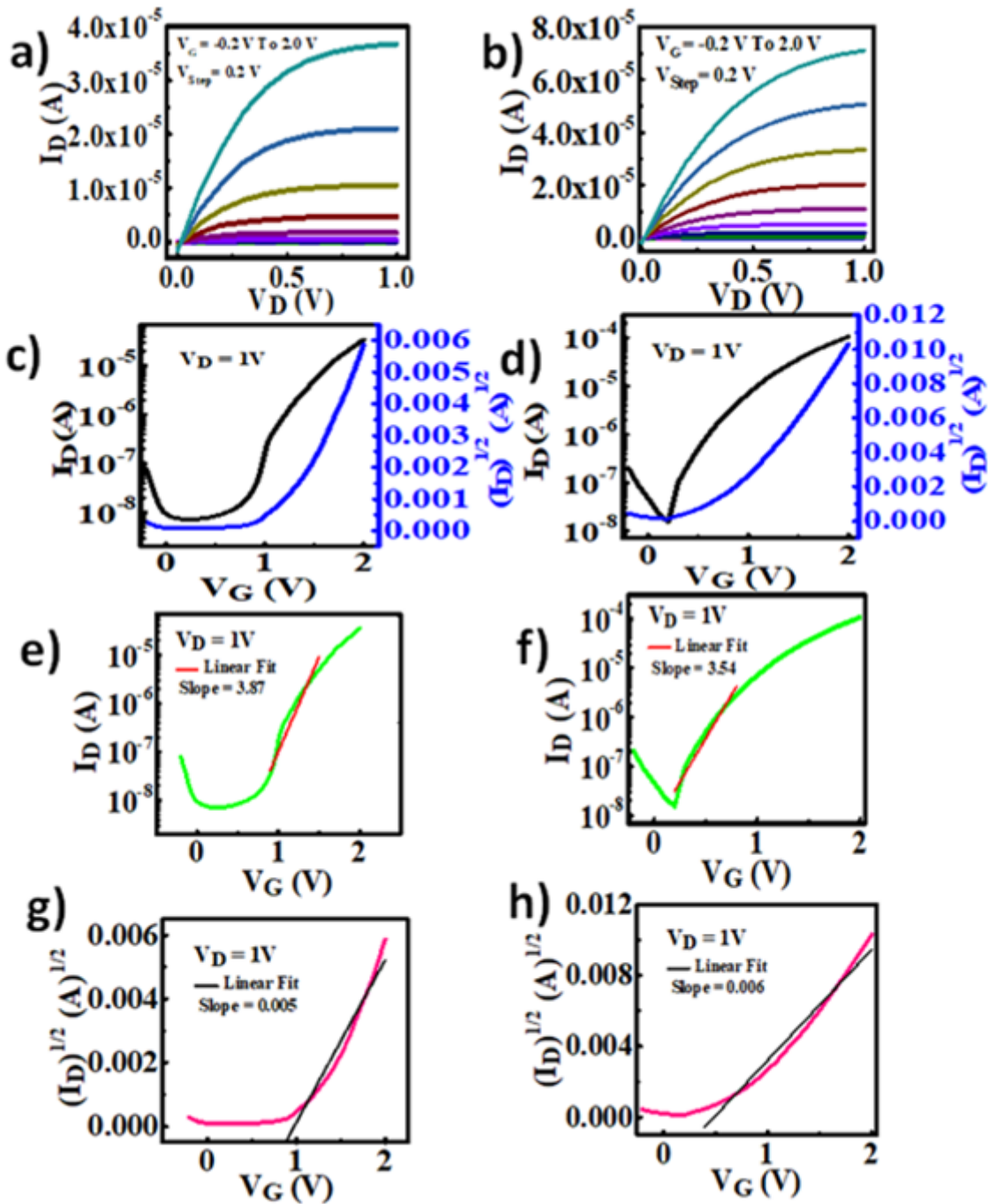


Figure 4

Variation of a) Leakage current density with applied voltage, and b) Areal capacitance with frequency for  $p^{++}\text{-Si/Li-Al}_2\text{O}_3\text{/Al}$  and  $p^{++}\text{-Si/TiO}_2\text{/Li-Al}_2\text{O}_3\text{/Al}$  MIM devices.



**Figure 5**

Transistor characterization of single layer and bilayer gate-dielectric SnO<sub>2</sub> TFT. a) and b) Output characteristics; c) and d) Transfer characteristics; e) and f) Linear fit of log( $I_D$ ) vs.  $V_G$  curve to extract SS value; g) and h) Linear fit of  $(I_D)^{1/2}$  vs.  $V_G$  to extract carrier mobility of Device 1 and Device 2, respectively.

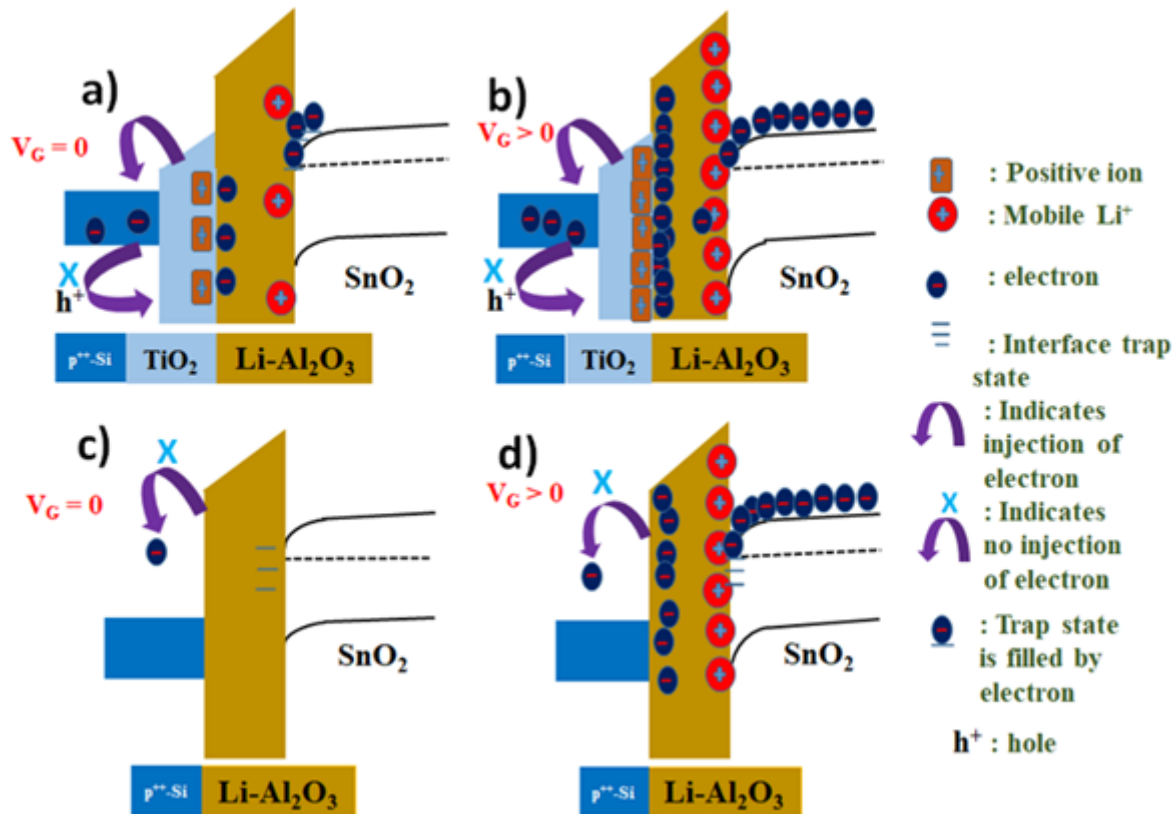


Figure 6

Metal-Insulator-Semiconductor structures illustrating the mechanism of variation in transistor performances with single layer and bilayer dielectric stack. Energy band diagram of a) and c) without applied bias, and b) and d) with applied positive bias of Device 2 with bilayer  $\text{TiO}_2/\text{Li-Al}_2\text{O}_3$  dielectric and Device 1 with single layer  $\text{Li-Al}_2\text{O}_3$  dielectric, respectively.